Research Article

Corrosion Inhibition and Thermodynamic Activation Parameters of Arcatium Lappa extract on Mild Steel in Acidic Medium

A. S. Fouda[*1], G. Y. El-Awady[1] and A. S. Abou-Salem[2]

[1]Chemistry Department, Faculty of Science, Mansoura University, Mansoura-35516, Egypt
[2]Protective Coatings, JOTUN, Egypt

Abstract

The effect of an aqueous extract of Arcatium Lappa on the corrosion behavior of mild steel in 1M HCl solution has been investigated by weight loss, potentiodynamic polarization, electrochemical impedance spectroscopy (EIS), and electrochemical frequency modulation techniques. The inhibition efficiency increased with increase in inhibitor concentration but deceased with rise in temperature. The thermodynamic parameters of corrosion and adsorption processes were calculated and discussed. The adsorption of this extract was found to obey Langmuir adsorption isotherm. The potentiodynamic polarization measurements indicated that the extract is of mixed type. The results obtained from the three different techniques were in good agreement.

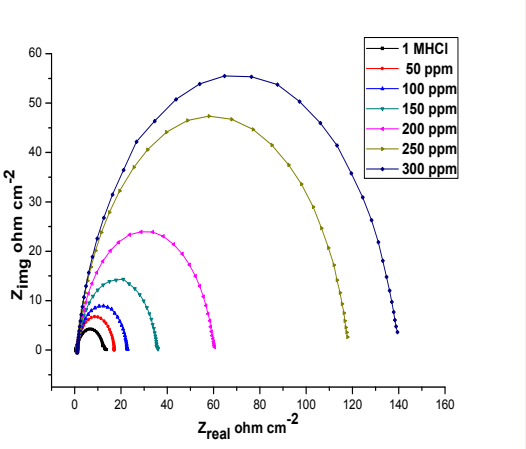

Keywords: Arcatium Lappa, corrosion inhibition, mild steel, adsorption

***Correspondence**
A. S. Fouda,
Email: asfouda@mans.edu.eg

Introduction

In oil fields hydrochloric acid solution is recommended as the cheapest way to dissolve calcium carbonate, $CaCO_3$, scale inside the pipelines under most conditions. Accordingly, corrosion inhibitors must be injected with the hydrochloric acid solution to avoid the destructive effect of acid on the surface of the pipe lines [1]. Mild steel has been widely employed as a construction material for pipe work in the oil and gas production such as down-hole tubular, flow lines and transmission pipelines [2]. Several studies have been published on the use of natural products as corrosion inhibitors in different media [3–11]. Most of the natural products are nontoxic, biodegradable and readily available in adequate quantities. Various parts of the plants, seeds [12, 13], fruits [14], leaves [15–17], and flowers [18–21] were extracted and used as corrosion inhibitors.

The aim of the present work is to find a naturally occurring, cheap and environmentally safe substance that could be used for inhibiting the corrosion of mild steel. The use of such substances will establish, simultaneously, the economic and environmental goals. In this piece of research, we report the inhibition action of Arcatium extract against the corrosion of mild steel in HCl solutions.

Experimental

Weight loss measurements

Coupons were prepared from mild steel sheet with a composition (in weight %) of C: 0.17–0.24, P: 0.04, Mn: 0.30–0.60, S: 0.05 and Fe: balance. Specimens cut with 4.0 cm X 2.0 cm X 0.15 cm dimensions were used for weight loss

measurements. The electrolyte was 1 M HCl solution prepared using double-distilled water. All chemicals were analytical-grade reagents. The extract was obtained by water infusion: a mass of about 5 g of dried and crushed leaves was added to a beaker containing 100 mL of bidistilled water that was freshly boiled and left to sit for 30 min off the heat; this mixture was agitated sporadically. After extraction, the sample was filtered, the volume was lyophilized, and the extract was stored in a desiccator until the time of analysis. The experiments were carried out under non-stirred and naturally aerated conditions. The concentration range of the Arcatium extract used was varied from 50 to 300 ppm, and 100 mL of electrolyte was used for each experiment. The addition of the Arcatium extract did not change the pH of the hydrochloric acid solution. After different immersion time (30, 60, 90, 120, 150 and180 min) the mild steel samples were taken out, washed with bidistilled water then dried. The weight loss was determined on an analytical balance with a precision of 0.1 mg. The weight loss values are used to calculate the corrosion rate (CR) in milli-meter per year (mmy^{-1}) by the relation:

$$CR = \frac{K \times \Delta W}{D \times A \times t} \quad (1)$$

Where, K is a constant and equals to $8.76X10^4$, ΔW is the weight loss (mg), D is the mild steel density (g/cm^3), A is the exposure area of the specimen (cm^2). Also, the degree of surface coverage (θ) and the surface Inhibition efficiency (%IE) was calculated from:

$$\%IE = \theta \times 100 = [1 - (\Delta W / \Delta W')] \times 100 \quad (2)$$

Where, ΔW and $\Delta W'$ are the weight losses in the presence and absence of inhibitor, respectively.

Electrochemical measurements

Electrochemical measurements were carried out using a conventional three-electrode cylindrical glass cell at a temperature of 25°C. The working electrode was a mild steel of above composition of 1 cm^2 area and the rest being covered by using commercially available epoxy resin. A saturated calomel electrode (SCE) and a platinum sheet (1 cm^2) were used as the reference and auxiliary electrodes, respectively. Before each experiment, the electrode was allowed to corrode freely, and its open circuit potential (OCP) was recorded as a function of time up to 30 min. After this time a steady-state potential was attained i.e. the E_{corr} of the working electrode, was obtained. EFM performed using two frequencies 2 and 5 Hz. The base frequency was 1 Hz. In this study, we use a perturbation signal with amplitude of 10 mV for both perturbation frequencies of 2 and 5 Hz. After that, electrochemical impedance measurements were carried out using AC signals of 10 mV amplitude peak-to-peak in the frequency range of 100 kHz to 5 mHz. The impedance diagrams are given in the Nyquist and Bode representation. Finally, anodic and cathodic polarization curves were obtained separately from -0.7 to 0.7 V at a scan rate 1 mVs^{-1}. The above procedures were repeated for each concentration of inhibitor. The electrochemical experiments were performed using a computer-controlled instrument, Gamry Instrument Series G750™ Potentiostat/Galvanostat/ZRA with a Gamry framework system based on ESA400. Gamry applications include software EIS300 for EIS, DC105 software for polarization, and EFM140 to calculate the corrosion current density and the Tafel constants for EFM measurements. A computer was used for collecting data. Echem Analyst 5.5 Software was used for plotting, graphing and fitting data. The corrosion penetration rate (CR) in millimeter per year (mm yr^{-1}) is calculated from the following equation [18]:

$$CR = [k \times a \times I / D \times V] \quad (4)$$

Where, k is a constant equals to 0.00327 when expressing corrosion penetration rate in millimeter per year (mm yr^{-1}), a is the atomic mass of Fe, I is the corrosion current density ($\mu A\ cm^{-2}$), D is the density of mild steel (g/cm^3), and V is the valence entered in the Tafel dialogue box. With: 3270 = 10 x [1 year (in seconds) / 96497.8] and 96497.8 =1Faraday in Coulombs. The % IE_p was calculated from:

$$\%IE_p = [1- (I^o_{corr} / I_{corr})] \times 100 \quad (5)$$

Where, I^o_{corr} and I_{corr} are the corrosion current densities of uninhibited and inhibited solution, respectively.

Surface analysis

The surface morphology and EDS analysis of mild steel specimens after weight loss measurements in 1 M HCl in the absence and presence of 300 ppm Arcatium Lappa extract were studied using scanning electron microscope (Jeol JSM-T20, Japan) equipped with an Oxford Inca energy dispersion spectrometer system. The working sample was analyzed at five different locations to ensure reproducibility.

Results and Discussion

Weight loss measurements

The weight loss of mild steel specimens immersed into 1 M HCl, in absence and presence of different concentration of Arcatium Lappa extract, was investigated after different immersion time (30-180 min) at different temperature (30-60°C) only weight-loss curve at 30°C illustrated in **Figure 1**. The %IE values at different temperature are shown in **Table 2**. The results show that the presence of Arcatium plant extract suppresses the corrosion rate of the mild steel specimens in 1M HCl solution. It was noted that the % IE increase with the plant extract concentration increases.

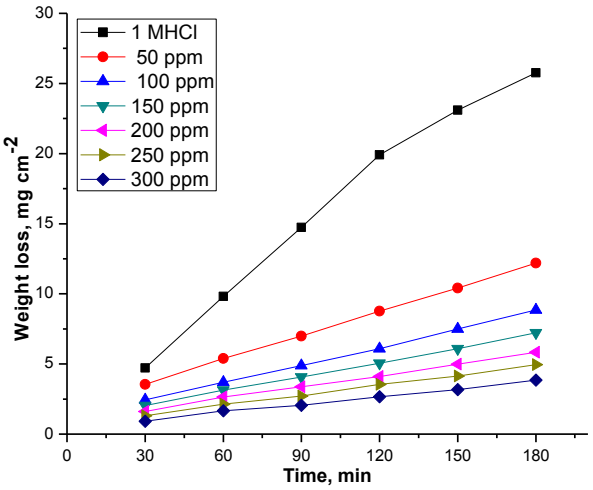

Figure 1 Weight Loss-time curve for the dissolution of mild steel in absence and presence of different concentrations of Arcatium extract at 30°C.

Table 1 The effect of different concentration of Arcatium extract on the corrosion rate (CR) (mg $cm^{-2}min^{-1}$) and inhibition efficiency (%IE) of mild steel in 1M HCl solution at different temperatures

$[C_{inh}]$ (ppm)	30°C		40 °C		50 °C		60°C	
	θ	%IE	θ	%IE	θ	%IE	θ	%IE
50	0.559	55.9	0.931	39.1	0.459	45.9	0.315	31.5
100	0.694	69.4	0.564	56.4	0.595	59.5	0.435	43.5
150	0.746	74.6	0.598	59.8	0.632	63.2	0.496	49.6
200	0.794	79.4	0.69	69.0	0.719	71.9	0.575	57.5

250	0.822	82.2	0.735	73.5	0.739	73.9	0.602	60.2
300	0.866	86.6	0.762	76.2	0.771	77.1	0.637	63.7

Adsorption isotherm

The values of surface coverage θ for different concentrations of the studied extract at different temperature have been used to explain the best isotherm to determine the adsorption process. The adsorption of inhibitor molecules on the surface of mild steel electrode is regarded as substitutional adsorption process between the organic compound in the aqueous phase (Org_{aq}) and the H_2O molecules adsorbed on the aluminum surface $(H_2O)_{ads}$ [22].

$$Org_{(sol)} + x\,(H_2O)_{ads} \rightarrow Org_{(ads)} + x\,H_2O_{(sol)} \quad (6)$$

Where, x is the size ratio, that is, the number of H_2O molecules replaced by one inhibitor molecule. Attempts were made to fit θ values to various isotherms including Frumkin, Langmuir, Temkin and Freundlich isotherms. By far the results were best fitted by Langmuir adsorption isotherm. Plotting C/θ against C gave a straight line with unit slop value **Figure (2)** indicating that the adsorption of inhibitor molecules on mild steel surface follows Langmuir adsorption isotherm. From these results one can postulates that there is no interaction between the adsorbed species.

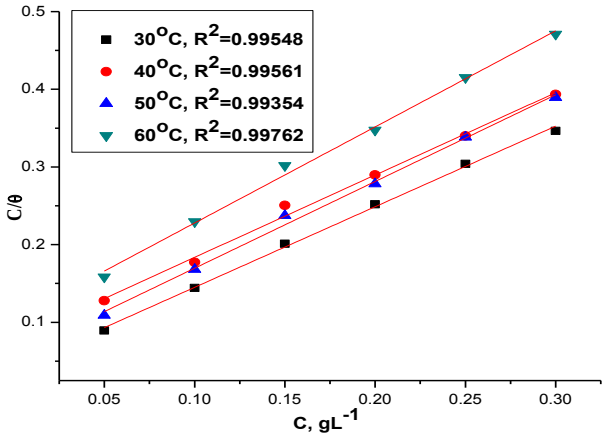

Figure 2 Curve fitting of corrosion data obtained from weight loss method for mild steel in 1 M HCl in the presence of different concentrations of the investigated plant extract to Langmuir adsorption isotherm at different temperature.

Effect of temperature

The effect of temperature on the rate of dissolution of mild in 1 M HCl containing different concentrations of the investigated inhibitor was tested by weight loss measurements over a temperature range from 30 to 60 °C. The effect of increasing temperature on the corrosion rate (k_{corr}) and %IE obtained from weight loss measurements. The results revealed that, on increasing temperature there is an increase of k_{corr} while %IE decreases for all compounds used. The activation energy (E_a) of the corrosion process was calculated using Arrhenius equation [23]:

$$k = A \exp(-E_a^*/RT) \quad (7)$$

Where, k is the rate of corrosion, A is Arrhenius constant, R is the gas constant and T is the absolute temperature.
Figure 3 represents Arrhenius plot (log k_{corr} vs. 1/T) for uninhibited and inhibited 1 M HCl containing different concentrations of the studied inhibitor. The values of E^*_a can be obtained from the slope of the straight lines. As in **Table 2** the increase of the activation energies in the presence of extract is attributed to an appreciable decrease in the

adsorption process of the extract on the metal surface with increase of temperature and a corresponding increase in the reaction rate because of the greater area of the metal that is exposed to the acid [24].

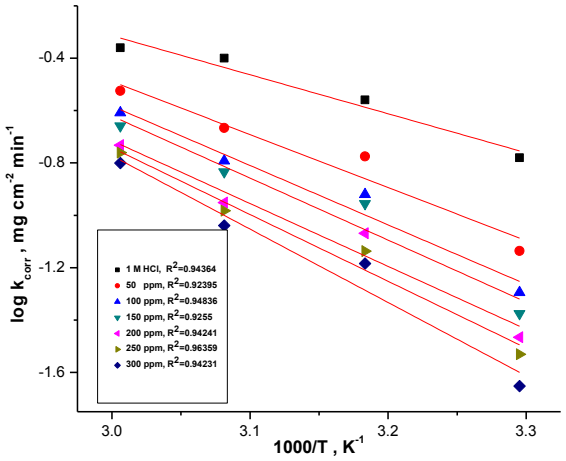

Figure 3 Arrhenius plots (log k vs 1/T) for mild steel in 1M HCl in the absence and presence of different concentration of Arcatium extract

The entropy of activation (ΔS^*) and the enthalpy of activation (ΔH^*) for dissolution of mild steel in 1 M HCl were obtained by applying the transition state equation:

$$\log k_{corr}/T = \log (R/ Nh + \Delta S^*/ 2.303R) + (-\Delta H^*/ 2.303RT) \quad (8)$$

Where, N is Avogadro's number, h is Planck's constant. A plot of log (k_{corr}/T) vs. (1 /T) **Figure 4** should give straight line with a slope = ($-\Delta H^*/2.303R$) and an intercept = log [(R/Nh) - ($\Delta S^*/2.303R$)]. The negative values of ΔS^* in the absence and presence of the inhibitors implies that the activated complex is the rate determining step and represents association rather than dissociation. It also reveals that an increase in the order takes place in going from reactants to the activated complex.

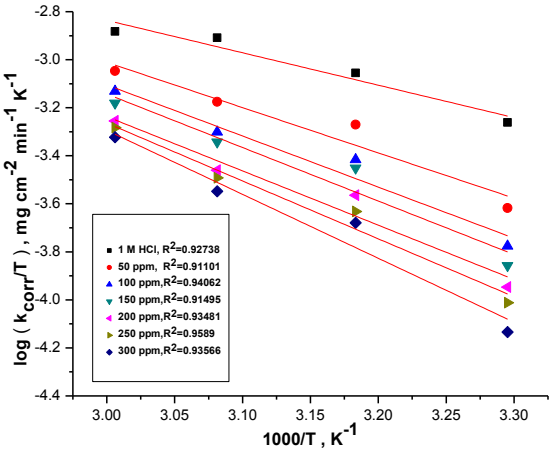

Figure 4 log (k_{corr}/T) vs (1/T) curves for mild steel in the absence and presence of different concentration of Arcatium Lappa extract

Table 2 Activation parameters for mild steel corrosion in the absence and presence of various concentrations of Arcatium Lappa extract in 1 M HCl

$[C_{inh}]$ (ppm)	E^*_a kJ mol^{-1}	ΔH^* kJ mol^{-1}	$-\Delta S^*$ J mol^{-1} K^{-1}
0	28.5	25.8	174.3
50	38.7	36.1	146.9
100	43.4	40.7	134.7
150	45.3	42.6	129.7
200	45.9	43.3	129.6
250	48.8	46.1	121.6
300	53.6	50.9	107.7

Potentiodynamic polarization technique

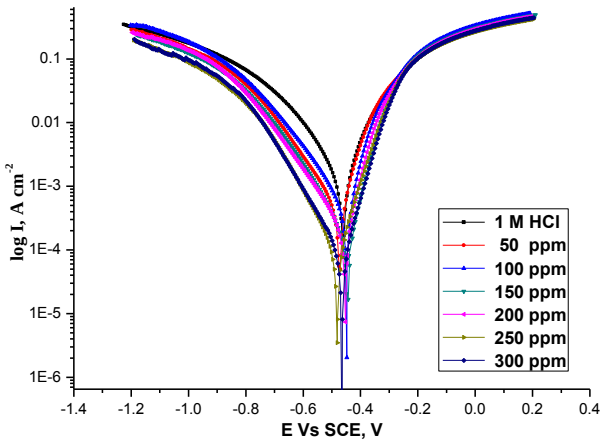

Figure 5 potentiodynamic polarization curves for the dissolution of mild steel in 1M HCl in the absence and presence of different concentrations of Arcatium Lappa extract at 25^{o}C

Figure 5 shows typical anodic and cathodic Tafel polarization curves for mild steel in 1 M HCl in absence and presence of various concentrations of Arcatium Lappa. The values of cathodic (β_c) and anodic (β_a) Tafel constants were calculated from the linear region of the polarization curves. The corrosion current density (I_{corr}) was determined from the intersection of the linear parts of the cathodic curves with the stationary corrosion potential (E_{corr}). The percentage inhibition efficiency (%IE) was calculated using the following equation:

$$IE\% = [1 - (I_{corr,\ add}/I_{corr,\ free})] \times 100 \qquad (9)$$

Where, $I_{corr,free}$ and $I_{corr,add}$ are the corrosion current densities in the absence and presence of inhibitors, respectively.

Table 3 shows the effect of the inhibitor concentrations on the corrosion kinetics parameters, such as β_a, β_c, E_{corr}, I_{corr} and %IE from the results given in Table 1 the following observation could be drawn:

(a) The Tafel lines are shifted to more positive and negative potential for anodic and cathodic processes, respectively, relative to the blank curve. This means that the plant extract influence both cathodic and anodic processes. However, the data suggested that the inhibitor acts mainly as mixed type inhibitor [25].
(b) The inhibitor molecules found in the aqueous extract decrease the surface area available for anodic dissolution and cathodic hydrogen evolution reaction without affecting the reaction mechanism.
(c) The values of E_{corr} change slowly to less negative values (i.e. nearly remain constant) and the values of I_{corr} decrease.
(d) The value of IEs increases indicating the inhibiting effect of these compounds.

Table 3 The effect of different concentration of Arcatium Lappa extract on the free corrosion potential (E_{corr}), corrosion current density (I_{corr}), Tafel slopes (β_a& β_c), inhibition efficiency (% IE) and corrosion rate (k_{corr}) for the corrosion of mild steel in 1M HCl at 30^{o}C

[C_{inh}] (ppm)	**i_{corr}, µA cm^{-2}**	**-E_{corr}, mV vs SCE**	**β_a, mV dec^{-1}**	**β_c, mV dec^{-1}**	**k_{corr} mpy**	**θ**	**IE%**
0	1750	461	110	195	801.1	----	----
50	560	473	85	173	255.9	0.680	68.0
100	526	448	73	171	240.5	0.699	69.9
150	213	453	64	156	97.5	0.878	87.8
200	183	446	68	150	83.5	0.895	89.5
250	108	481	77	132	49.5	0.938	93.8
300	88.1	465	70	133	40.2	0.946	94.6

Electrochemical impedance spectroscopy

The corrosion of mild steel in 1M HCl in the presence of studied plant extract was investigated by EIS method at 30^{o}C after 20 min. immersion. Nyquist and Bode plots in the absence and presence of investigated extract is present in **Figures (6)** and **(7)**; respectively. It is apparent that all Nyquist plots show a single capacitive loop, both in uninhibited and inhibited solutions. The impedance data of mild steel in 1 M HCl are analyzed in terms of an equivalent circuit model **Figure (8)** which includes the solution resistance R_s or R_Ω and the double layer capacitance C_{dl} which is placed in parallel to the charge transfer resistance R_{ct} [26] due to the charge transfer reaction. The higher (R_{ct}) values, are generally associated with slower corroding system [27-28]. The values of %IE were calculated by the equation as follows:

$$IE\% = [1-R_{ct}/R_{ct\,(inh)}] \times 100 \qquad (10)$$

Where, R_{ct} and $R_{ct\,(inh)}$ are charge-transfer resistance values in the absence and presence of the inhibitor, respectively. For the Nyquist plots it is obvious that low frequency data are on the right side of the plot and higher frequencies are on the left. This true for EIS data where impedance usually falls as frequency rises (this is not true of all circuit). In the Bode plot, the impedance is plotted with log frequency on the x-axis and both the log of absolute value of the impedance and the phase shift on the y-axis. Unlike the Nyquist plot, the phase angle does not reach 90^o as it would for pure capacitive impedance. In the Bode plot at the highest frequencies, log R_s appears as a horizontal plateau while at the lowest frequencies, log (R_s + R_{ct}) appears as a horizontal plateau. The capacity of double layer (C_{dl}) can be calculated from the following equation:

$$C_{dl} = 1/ (2\pi f_{max} R_{ct}) \qquad (11)$$

Where, f_{max} is the maximum frequency. The parameters obtained from impedance measurements are given in **Table 4**. It can be seen that the value of charge transfer resistance increases with extract concentration [29] also the % IE increases as the phase angle increases. The impedance study confirms the inhibiting characters of the investigated

extract obtained with potentiostatic polarization methods. These observations show that the extract is adsorbed on mild steel surface. It is generally, assumed that adsorption at the metal-solution interface is the first step in the inhibition mechanism in aggressive acidic media. Four mechanisms have been suggested for the adsorption of organic molecules at the metal-solution interface [30].

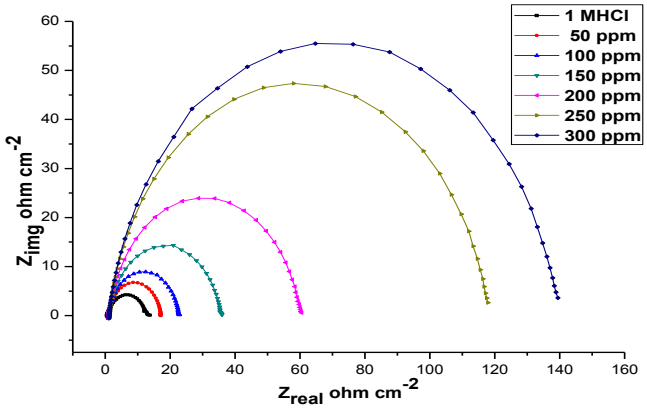

Figure 6 Nyquist plots showing effect of increasing concentration of Arcatium extract on corrosion of mild steel in HCl solutions

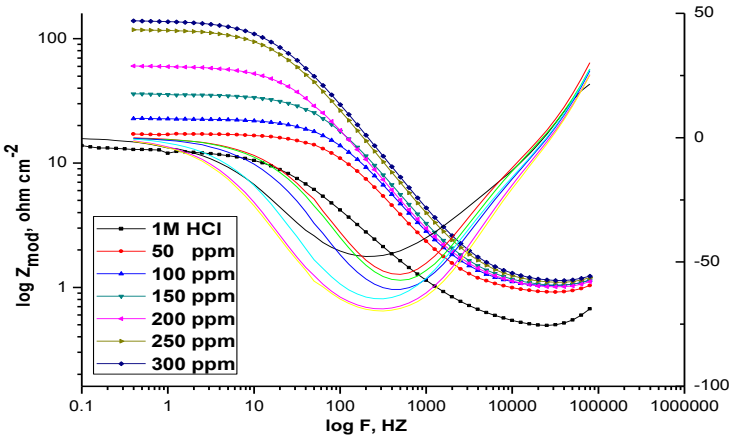

Figure 7 Bode plot for corrosion of mild steel in 1M HCl in the absence and presence of different concentrations of Arcatium extract at 25°C

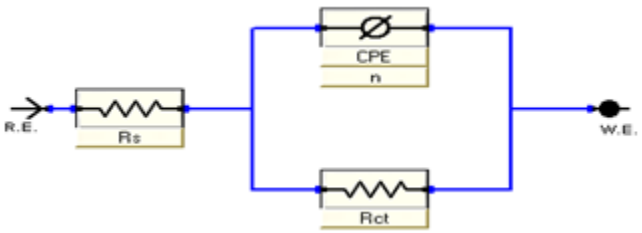

Figure 8 Equivalent circuit model used to fit the impedance spectra

Table 4 Data from electrochemical impedance measurements for corrosion of mild steel in 1 M HCl solutions at various concentrations of Arcatium extract.

$[C_{inh}]$ ppm	R_{ct}, Ohm cm^2	C_{dl}, $\mu F cm^{-2}$	% IE
0	12.45	8.33	---
50	16.06	52.60	22.4
100	21.43	48.72	41.9
150	34.28	34.33	63.7
200	58.55	16.56	78.7
250	114.9	12.33	89.2
300	135.7	11.60	90.8

Electrochemical Frequency Modulation (EFM) measurements

Electrochemical frequency modulation is a non-destructive corrosion measurement technique that can directly give values of the corrosion current without prior knowledge of Tafel constants. Like EIS, it is a small signal ac technique. Unlike EIS, however, two sine waves (at different frequencies) are applied to the cell simultaneously. Because current is a non-linear function of potential, the system responds in a non-linear way to the potential excitation. The current response contains not only the input frequencies, but also contains frequency components which are the sum, difference, and multiples of the two input frequencies. The two frequencies may not be chosen at random. They must both be small, integer multiples of a base frequency that determines the length of the experiment. **Figures (9, 10)** show representative examples for the intermodulation spectra obtained from EFM measurements in absence and presence of different concentrations of the extract. Each spectrum is a current response as a function of frequency. It is important to note that between the peaks the current response is very small. There is nearly no response (<100 nA) at 4.5 Hz, for example, the frequencies and amplitudes of the peaks are not coincidences. They are direct consequences of the EFM theory [31, 32]. Corrosion kinetic parameters are listed in **Table 5.**

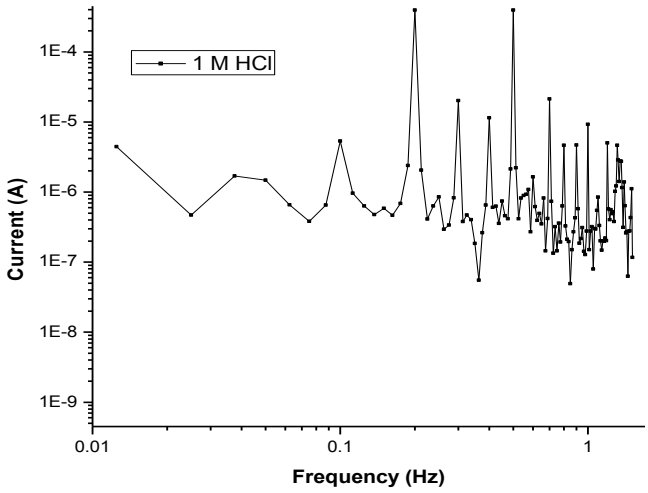

Figure 9 Intermodulation spectrum recorded for mild steel in 1 M HCl at 25˚C

The inhibition efficiency values were calculated from the following equation:

$$\%IE = [1- (I_{corr}/I^{o}_{corr})] \times 100 \quad (12)$$

Where, I^{o}_{corr} and I_{corr} are corrosion current densities in the absence and presence of the inhibitor, respectively. The great strength of the EFM is the causality factors which serve as an internal check on the validity of the EFM measurement [32]. With the causality factors the experimental EFM data can be verified. The causality factors in **Table 5**, which are compatible with to theoretical values according to the EFM theory [31], should guarantee the validity of Tafel slopes and corrosion current densities. The standard values for CF-2 and CF-3 are 2.0 and 3.0, respectively [31]. It is quite obvious that the data obtained from chemical and electrochemical measurements were in a good agreement with the results obtained from EFM technique.

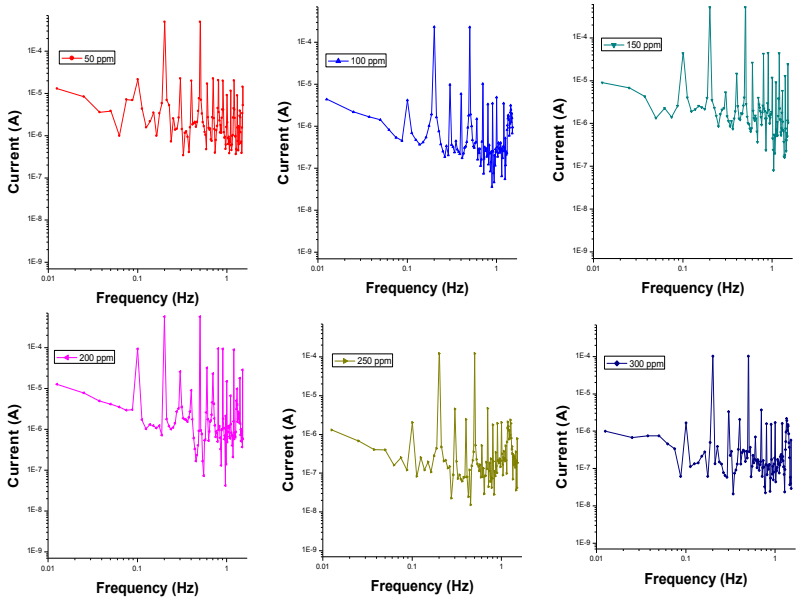

Figure 10 Intermodulation spectrum for recorded for mild steel in 1M HCl in the presence of various concentrations (50-300 ppm) of Arcatium Lappa extract at 25˚C

Table 5 Electrochemical kinetic parameters obtained by EFM technique for mild steel in 1M HCl solutions containing various concentrations of the Arcatium Lappa extract at 25˚ C

$[C_{inh}]$ (ppm)	I_{corr}, µA cm^{-2}	β_a, mV dec^{-1}	β_c, mV dec^{-1}	CF 2	CF 3	C.R mpy	θ	% IE
Blank	655.7	92	131	2.06	3.5	299.6		
50	431.7	53	62	1.57	1.3	197.2	0.34	34
100	337.3	83	107	1.87	3.341	154.1	0.485	48.5
150	321.6	39	40	354.6	1.762	147	0.509	50.9
200	256.6	28	29	2.058	3.067	117.2	0.608	60.8
250	182.9	88	110	2.041	2.72	83.56	0.721	72.1
300	147.9	85	104	1.872	2.508	67.6	0.774	77.4

Scanning Electron Microscopy (SEM) Studies

The morphology of the surface of the corroded mild steel samples was studied using SEM after immersion in 1M HCl for 12 h. **Figure (11-a)** shows the surface of pure mild steel. **Figure (11b-c)** represents the micrographs of mild steel in 1M HCl in absence and presence of 300 ppm of Arcatium Lappa extract. From **Figure (11-b)**, the micrographs show an extensive etching composed of dark areas. In presence of 300 ppm of the investigated extract, a protective film is formed on the surface of mild steel as shown in **Figure (11-c)**. This film appears to be smooth and covers the whole surface of the sample without minor flaw. These features confirm the high % IE obtained for Arcatium Lappa extract.

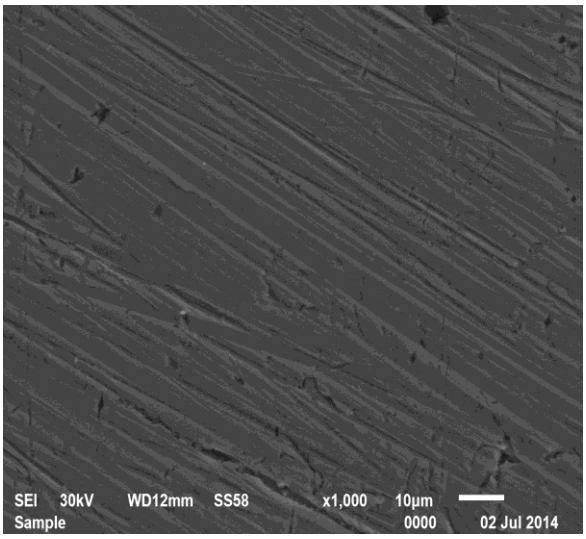

Figure 11(a) Pure mild steel

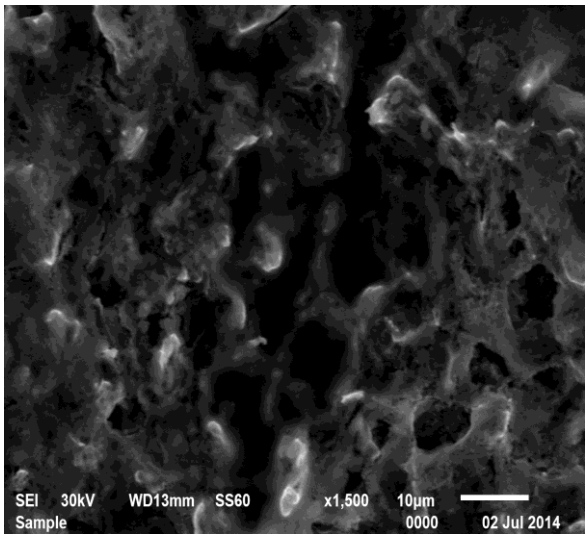

Figure 11(b) 1 M HCl

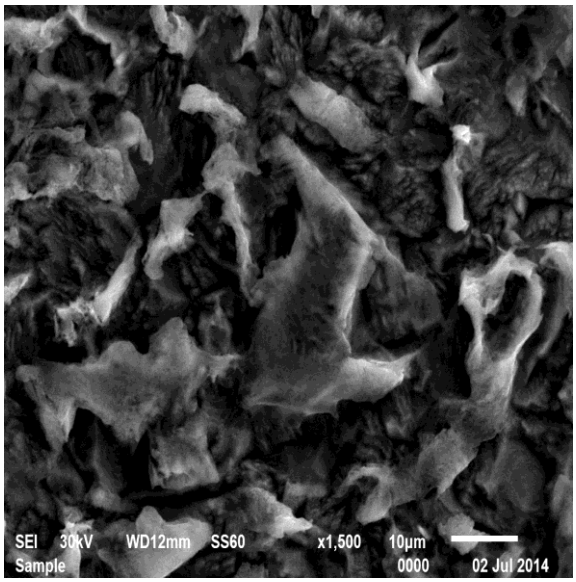

Figure 11(c) 1 M HCl +300 ppm Arcatium Lappa

Figure 11 SEM micrographs for mild steel in absence and presence of 300 ppm of Arcatium Lappa extract

Energy Dispersion Spectroscopy (EDX) Studies

The goal of this section was to confirm the results obtained from chemical and electrochemical measurements that a protective surface film of inhibitor is formed on the electrode surface. The corresponding Energy dispersive X-ray (EDX) profile analysis is presented in **Figure (12)**. The EDX survey spectra were used to determine which elements of extract components were present on the electrode surface before and after exposure to the extract solution. For the specimen without exposure to acid solution and inhibitor treatment **Figure (12-a)** Fe with small traces of Mn, Si, C was detected **(Table 6).** It is noticed the existence of the carbon, oxygen peak in the EDX spectra in the case of the sample exposed to the extract, could be attributed to the adsorption of organic molecules at the mild steel surface. The spectra of **Figure (12–c)** shows that the Fe peaks are considerably suppressed relative to the samples prepared in 1 M HCl solution, and this suppression increases with increasing the extract concentration and immersion time. The suppression of the Fe lines occurs because of the overlying extract film. These results confirm those from polarization measurements which suggest that a surface film inhibited the metal dissolution, and hence retarded the hydrogen evolution reaction. This surface film also increases the charge-transfer resistance of the anodic dissolution of mild steel, as present as before in **Table 4**, slowing down the corrosion rate. Therefore, EDX examinations of the electrode surface support the results obtained from chemical and electrochemical methods that Arcatium Lappa extract is a good inhibitor for mild steel corrosion in HCl solutions.

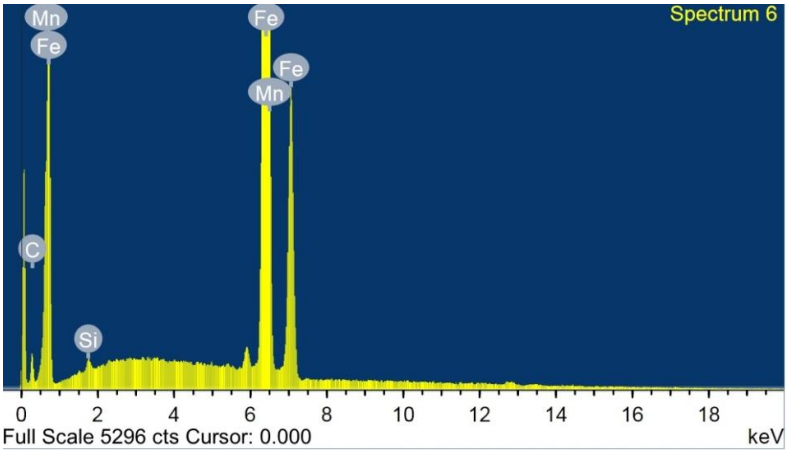

(a) Pure mild steel

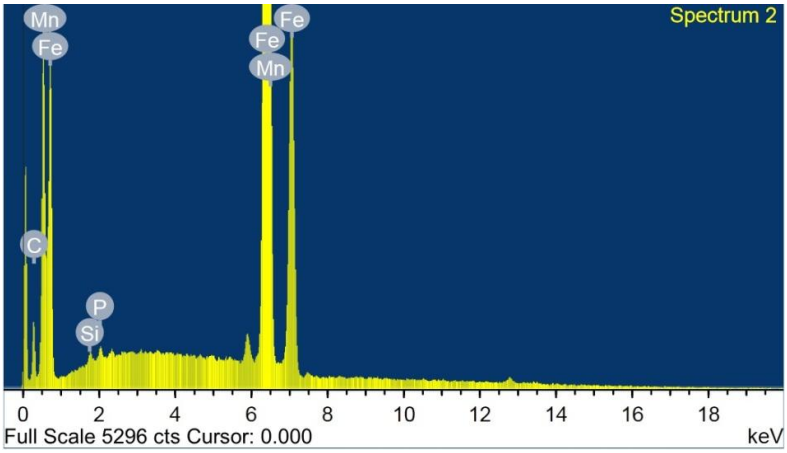

(b) 1 M HCl only

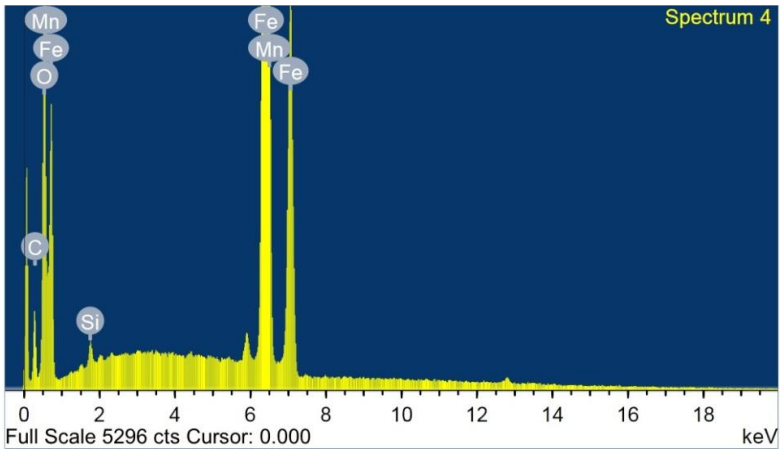

(c) 1 M HCl +300 ppm Arcatium Lappa

Figure 12 EDX analysis on mild steel in absence and presence of 300 ppm of Arcatium extract for 12 hrs immersion

Table 6 Surface composition (weight %) of mild steel after 12 hrs. of immersion in HCl without and with the optimum concentration of the studied inhibitor

Mass %	Fe	C	O	Si	Mn
Pure	87.72	11.59	-	0.38	0.76
Blank	82.06	12.66	-	0.26	0.74
300 ppm	64.46	16.68	21.9	0.42	0.27

Conclusions

Weight loss, polarization, impedance and EFM were used to study the corrosion inhibition of mild steel in 1 M HCl solutions using aqueous extract of Arcatium Lappa as an environmentally safe inhibitor. The principle conclusions are:

1. The acid corrosion of mild steel is reduced upon the addition of Arcatium Lappa extract and inhibition efficiency increases with increasing the plant extract concentration.
2. A surface film of extract is formed on the electrode surface via electrostatic adsorption.
3. EDX observations of the electrode surface showed that a surface film of the extract is formed on the electrode surface. This film retarded the reduction of H^+ ions and inhibited metal dissolution in hydrochloric acid solutions (mixed-type inhibitor).
4. Physisorption is proposed as the mechanism for corrosion inhibition.
5. The inhibition efficiencies obtained from weight loss data are comparable with those obtained from polarization, EIS and EFM measurements.

References

[1] J.E. Oddo, M.B. Tomson, J. Pet. Tech. (1982) 1583.
[2] B. Ridd, T.J. Blakset, D. Queen, Corrosion, NACE, Paper No (78), Houston, Texas, 1998.
[3] A.K. Satapathy, G. Gunasekaran, S.C. Sahoo, Kumar Amit, P.V. Rodrigues, Corros.Sci. 51 (2009)2848–2856.
[4] A.M. Abdel-Gaber, E. Khamis, H. Abo-ElDahab, Sh. Adeel, Mater. Chem. Phys.109 (2008) 297–305.
[5] A.M. Abdel-Gaber, Int. J. Appl. Chem. 3 (2007) 161–167.

[6] R. Saratha, V.G. Vasudha, J. Chem. 6 (2009) 1003–1008.
[7] O.K. Abiola, A.O. James, Corros. Sci. 52 (2010) 661–664.
[8] A.M. Abdel-Gaber, B.A. Abd-El-Nabey, M. Saadawy, Corros. Sci. 51 (2009)1038–1042
[9] J.C. da Rocha, N.D.C. Ponciano Gomes, E. D'Elia, Corros. Sci. 52 (2010) 2341–2348.
[10] R. Kanojia, G. Singh, Surf. Eng. 21 (2005) 180–186.
[11] A. Ostovari, S.M. Hoseinieh, M. Peikari, S.R. Shadizadeh, S.J. Hashemi, Corros.Sci. 51 (2009) 1935–1949.
[12] [12] R.M. Saleh, A.A. Ismail, A.A. El Hosary, Corros. Sci. 23 (1983) 1239–1241.
[13] F. Zucchi, I.H. Omar, Surf. Technol. 24 (1985) 391–399.
[14] I.H. Farooqi, M.A. Quraishi, P.A. Saini, Corros. Prev. Control 46 (1999) 93–96.
[15] I. Ithaya Kumar, G. Udayabanu, N.S. Rawat, in: Proceedinggs of the Seventh European Symposium on Corrosion Inhibitors, Ann. Univ. Ferrara (1990) 735.
[16] A.A. El-Hosary, R.M. Salah, H.A. El-Dahan, in: Proceedings of the Seventh European Symposium on Corrosion Inhibitors, Ann. Univ. Ferrara (1990) 725.
[17] M. Kliškic´, J. Radoševic, S. Gudic, V. Katalinic, J. Appl. Electro. Chem. 30 (2000)823–830.
[18] A. Minhaj, P.A. Saini, M.A. Quraishi, I.H. Farooqi, Corros. Prev. Control 46 (1999)32–38.
[19] K. Srivastava, P. Srivastava, Corros. Prev. Control 27 (1980) 5.
[20] R.M. Saleh, A.A. Ismail, A.A. El Hosary, Corros. Prev. Control 31 (1984) 21–23.
[21] A.A. El Hosary, R.M. Saleh, A.M. Shams El Din, Corros. Sci. 12 (1972) 897–904.
[22] G. Moretti, G. Quartarone, A. Tassan, A. Zingales,Werkst. Korros. 45 (1994) 641.
[23] I. Putilova, S. Balezin, V. Barannik, Effect of azole compounds on corrosion of copper in acid medium, Metallic Corrosion Inhibitors, Pergamon, Oxford, 1960
[24] I.N. Putilova, S.A. Balezin, V.P. Barannik, T. Baba, Corros.Sci. 36 (1994) 79.
[25] L. Larabi, O.Benali, SM.Mekelleche, Y.Harek,,J.Appl Surf Sci., 253(2006):1371
[26] C.S. Hsu, F. Mansfeld, Corrosion 57 (2001) 747
[27] I. Epelboin, M. Keddam, H. Takenouti, J. Appl. Electrocehm.2 (1972)71-79
[28] M.Lagrenee, B. Mernari, B. Bounais, M. Traisnel, F. Bentiss, Corros. Sci. 44(2002)573
[29] Schweinsberg, D.; George, G.; Nanayakara, A.; Steiner, D.; Corros.Sci. 28 (1988)33.
[30] R.W. Bosch, J. Hubrecht, W.F. Bogaerts, B.C. Syrett, Corrosion 57 (2001) 60-70
[31] R.W. Bosch, W.F. Bogaerts, Corrosion 52 (1996) 204.

Publication History
Received 04th Dec 2014
Revised 12th Dec 2014
Accepted 19th Dec 2014
Online 30th Dec 2014